Hydrogen Bonding Interaction between the Primary Quinone Acceptor Q_A and a Histidine Side Chain in Photosystem II As Revealed by Fourier Transform Infrared Spectroscopy†

Takumi Noguchi,*,‡ Yorinao Inoue,‡ and Xiao-Song Tang§

Photosynthesis Research Laboratory, The Institute of Physical and Chemical Research (RIKEN), Wako, Saitama 351-0198, Japan, and Life Sciences Enterprise, E. I. du Pont de Nemours & Company, Wilmington, Delaware 19880-0173

Received September 23, 1998; Revised Manuscript Received October 28, 1998

ABSTRACT: Interactions of the primary quinone acceptor Q_A of photosystem II (PS II) with surrounding amino acid residues were studied by analysis of FTIR difference spectra of Q_A upon its photoreduction (Q_A^-/Q_A). Structural coupling with a His side chain was revealed by identifying the imidazole bands in the Q_A^-/Q_A spectrum using the PS II core complexes from *Synechocystis* PCC 6803 in which both of the two imodazole nitrogens of His side chains were specifically labeled with ^{15}N. Strong hydrogen bonding of the imidazole NH was shown by (i) the presence of several peaks at 2600−3000 cm^{-1}, which arise from Fermi resonance of harmonics or combinations of imidazole ring modes with the hydrogen bonding NH stretching vibration, and (ii) the 1179 cm^{-1} band, which can be assigned to the mode including NH deformation, is at a frequency significantly higher than the corresponding 1151 cm^{-1} band of model compounds 4- and 5-methylimidazole in aqueous solution. Also, the presence of the bands specific to the N_π-protonated state at 1109/1102/1090 and 1359 cm^{-1} suggests that the Q_A-coupled His is protonated at the N_π site. These results are in good agreement with the model of Q_A interaction in which His215 (D2), which coordinates to the non-heme iron at N_τ, is hydrogen bonded to the Q_A carbonyl through the N_π−H bond. In contrast, no bands of Trp side chains were detected in the Q_A^-/Q_A spectrum upon labeling of the indole ring of Trp residues with indole-d_5. This result indicates that Trp254 (D2), which corresponds to Trp252 (M) of the bacterial reaction center that is located in van der Waals contact with Q_A, is not strongly coupled with Q_A in PS II. Probably, the predicted $\pi-\pi$ interaction is not strong enough to influence the vibrations of the indole ring of Trp upon Q_A reduction, or Trp254 (D2) is located rather far from Q_A in PS II.

On the electron acceptor side of photosystem II (PS II[1]), an electron that is ejected from the photoexcited P680 is transferred to the primary quinone acceptor Q_A through a pheophytin cofactor. The resultant semiquinone anion radical Q_A^- further reduces the secondary quinone acceptor Q_B. Double reduction of Q_B by two electron transfer steps is followed by the proton uptake to produce a quinol (QH_2), which is then dissociated from the Q_B binding pocket of the PS II protein (*1*). This quinone reduction process of PS II closely resembles that of the reaction center of purple photosynthetic bacteria, whose structure has been clarified by X-ray crystallography. In *Rhodobacter spaeroides*, two carbonyl oxygens of Q_A are hydrogen bonded to the peptide nitrogen of Ala260 (M) and to the imidazole nitrogen of His219 (M), and Trp252 (M) is located parallel to the Q_A plane at a distance that suggests $\pi-\pi$ interaction (*2*, *3*). The structure of the Q_A binding site of PS II is expected to resemble that of purple bacteria on the basis of the conservation of His215 and Trp254 on the D2 subunit (*4*). In the absence of the X-ray structure of PS II, however, interaction of Q_A with the surrounding protein has been a target of spectroscopic studies.

The magnetic coupling of the Q_A^- semiquinone radical with surrounding nuclei has been investigated by ESEEM and ENDOR measurements. In native PS II, the magnetic interaction of Q_A^- with the nearby Fe^{2+}, which causes fast spin−lattice relaxation and the excessive broadening of the EPR signal, prevents studies using these techniques. Some decoupling methods that include modifying the non-heme iron center have been developed, i.e., depletion of the non-heme iron (*5*, *6*), substitution by diamagnetic Zn^{2+} (*7*), and conversion of the high-spin Fe^{2+} to the low-spin state by cyanide treatment (*8*) and high-pH (pH 11) treatment (*9*). All the ESEEM studies using these modified PS II samples have agreed on the coupling of Q_A^- with the peptide nitrogen (*9*−*15*). With regard to the coupling with the imidazole

† This research was supported by grants for the Photosynthetic Sciences and Biodesign Research Program at The Institute of Physical and Chemical Research (RIKEN) provided by the Science and Technology Agency (STA) of Japan, and was partially supported by the Central R&D Department of E. I. du Pont de Nemours & Co. (contribution 7846).

* To whom correspondence should be addressed.

‡ The Institute of Physical and Chemical Research.

§ E. I. du Pont de Nemours & Co.

[1] Abbreviations: DCMU, 3-(3,4-dichlorophenyl)-1,1-dimethylurea; ENDOR, electron nuclear double resonance; EPR, electron paramagnetic resonance; ESEEM, electron spin-echo envelope modulation; FTIR, Fourier transform infrared; 4- and 5-MeIm, 4- and 5-methylimidazole, respectively; Mes, 2-(*N*-morpholino)ethanesulfonic acid; IR, infrared; PS II, photosystem II; Q_A, primary quinone electron acceptor of PS II; Q_B, secondary quinone electron acceptor of PS II.

10.1021/bi982294v CCC: $18.00 © 1999 American Chemical Society
Published on Web 12/10/1998

nitrogen of a His side chain, the coupling has been found in non-heme iron-depleted, Zn^{2+}-substituted, and high-pH-treated PS II (*9*, *11*, *12*, *14*, *15)*, whereas early studies using cyanide-treated PS II (*10*, *11*, *13*, *14)* could not detect the coupling. Recently, this discrepancy was rationalized by detection of signals from an imidazole nitrogen with a considerably small hyperfine interaction constant in the cyanide-treated PS II preparation (*15*). The definite conclusion of the coupling with an imidazole nitrogen, however, awaits assignment of the ESEEM signals by specific isotope substitution of His residues in PS II complexes. ENDOR studies using non-heme iron-depleted (*6*) and cyanide-treated PS II (*16*) have shown two different hydrogen bonds in Q_A^-. The $\pi-\pi$ interaction with Trp254 (D2) has also been suggested from interpretation of the ENDOR data of non-heme iron-depleted PS II (*6*).

Although ESEEM and ENDOR spectroscopies are suitable methods for studying the coupling of Q_A^- with surrounding molecules, there is always a concern about modification of the Q_A^- environment by procedures of decoupling with the non-heme iron. Therefore, study of the Q_A interaction with other methods that do not require special treatment of the sample is urged. FTIR difference spectroscopy is the most promising method for achieving this goal. By detection of IR absorption changes upon photoreduction of Q_A in combination with selective isotope labeling of amino acid residues, molecular interactions of Q_A with specific amino acid side chains can be studied in the "native" PS II sample. Light-induced Q_A^-/Q_A difference spectra were previously obtained using PS II membranes from spinach (*17*, *18*) and carefully identified with control EPR measurements (*19*). In this study, we have studied the interaction of Q_A with His and Trp residues by FTIR spectroscopy using PS II core complexes from the cyanobacterium *Synechocystis* PCC 6803 in which His or Trp side chains are specifically isotope-labeled.

MATERIALS AND METHODS

Cells of the wild-type *Synechocystis* 6803 strain were grown photoautotrophically in BG-11 medium at 30 °C for 5 days in 10 L carboys using cool-white fluorescent lamps (7 W/m^2). The growth medium was bubbled with 5% CO_2 in air. Labeling (>90%) of *Synechocystis* cells with [^{15}N]-histidine (imidazole $^{15}N_\pi$ and $^{15}N_\tau$) was carried out following the methods of Tang et al. (*20*). To specifically deuterate tryptophan, *Synechocystis* cells were grown photoautotrophically in BG-11 medium containing 0.5 mM phenylalanine, 0.25 mM tyrosine, and 0.25 mM tryptophan-d_5 (hydrogen atoms of the indole ring are replaced with ^{2}H). Under such growth conditions, *Synechocystis* 6803 is a functional autotroph for the aromatic amino acids (*21*). PS II core complexes from *Synechocystis* were purified according to the procedure described earlier (*22*) and suspended in 50 mM Mes/NaOH (pH 6.0) buffer containing 20% (w/v) glycerol, 5 mM $MgCl_2$, 5 mM $CaCl_2$, and 0.03% dodecyl maltoside. Before the FTIR measurements, the core complexes were resuspended in 4 mM Mes/NaOH (pH 6.0) buffer containing 40 mM sucrose and 2 mM NaCl and treated with 10 mM NH_2OH to deplete the Mn cluster. NH_2OH in the buffer also works as an exogenous electron donor during photoaccumulation of Q_A^-. DCMU (0.1 mM) was added to the sample to block the electron flow beyond Q_A. The core suspension was then concentrated to about 6 mg of chlorophyll/mL using a Microcon-100 (Amicon). An aliquot of the concentrated sample (4−5 μL) was lightly dried on a BaF_2 plate under a N_2 gas flow and then covered with another BaF_2 plate.

FTIR spectra were measured on a JEOL JIR-6500 spectrophotometer equipped with an MCT detector (EG&G JUDSON IR-DET101). For PS II samples, the temperature was adjusted to 250 K in a liquid N_2 cryostat (Oxford model DN1704). Light-induced difference spectra were obtained by subtraction between the two single-beam spectra (150 s accumulation for each) measured before and after illumination for 5 s. A halogen lamp equipped with heat-cut and red (>600 nm) filters (~20 mW/cm^2 at the sample) was used for illumination. FTIR spectra of 4- and 5-methylimidazole (MeIm) dissolved in water (0.5 M) were measured at room temperature. The spectrum of water was measured and subtracted from the 4- and 5-MeIm spectra to cancel the large background created by water absorption. All the spectra were measured at 4 cm^{-1} resolution.

RESULTS

Figure 1a shows an FTIR difference spectrum of Q_A upon its photoreduction (Q_A^-/Q_A) measured at 250 K with the Mn-depleted PS II core complexes from *Synechocystis* PCC 6803. The sample included NH_2OH as an exogenous electron donor and DCMU as an inhibitor of electron flow beyond Q_A. Overall features of this Q_A^-/Q_A spectrum of the *Synechocystis* core are very similar to those of the previously reported Q_A^-/Q_A spectrum of PS II membranes of spinach (*17*−*19*). In particular, the main peak at 1478 cm^{-1} due to the CO stretching mode of the semiquinone anion remains unchanged, indicating that CO interaction of Q_A^- is virtually identical between *Synechocystis* and spinach. Some differences are seen in the amide I region of protein backbones at 1600−1700 cm^{-1}; negative peaks at 1658 and 1691 cm^{-1} and a positive peak at 1678 cm^{-1} (Figure 1a) are more pronounced in the *Synechocystis* core, and positive peaks at 1625 and 1660 cm^{-1} in spinach PS II membranes (*17*−*19*) are diminished in *Synechocystis*. These differences might be due to some changes of protein conformation around Q_A in the core complex (*Synechocystis*) from the membrane sample (spinach) or merely due to the difference between cyanobacteria and higher plants.

Figure 1b shows a Q_A^-/Q_A FTIR spectrum measured with PS II core complexes from *Synechocystis* cells in which both of the two imidazole nitrogens (N_τ and N_π) of His side chains are selectively labeled with ^{15}N. The spectrum seems almost identical with that of the unlabeled core (Figure 1a), although with a closer look there are some small changes. To abstract these changes, a difference spectrum between unlabeled and [^{15}N]His-labeled Q_A^-/Q_A (spectrum b − a) was obtained (Figure 1c). Subtraction was performed to cancel as many bands as possible. Bands are clearly observed in this double difference spectrum at 1474/1456/1444, 1359, 1256/1249, 1179/1169, 1109/1102/1090, 983/968, and 942 cm^{-1}. Structures around 1650 and 1550 cm^{-1} may be explained by the higher noise level in this region due to the presence of the major bands (amide I and II bands, respectively) in the original FTIR spectrum of the core complex.

The above bands sensitive to [^{15}N]His labeling should arise from the vibrational modes of the His side chain structurally

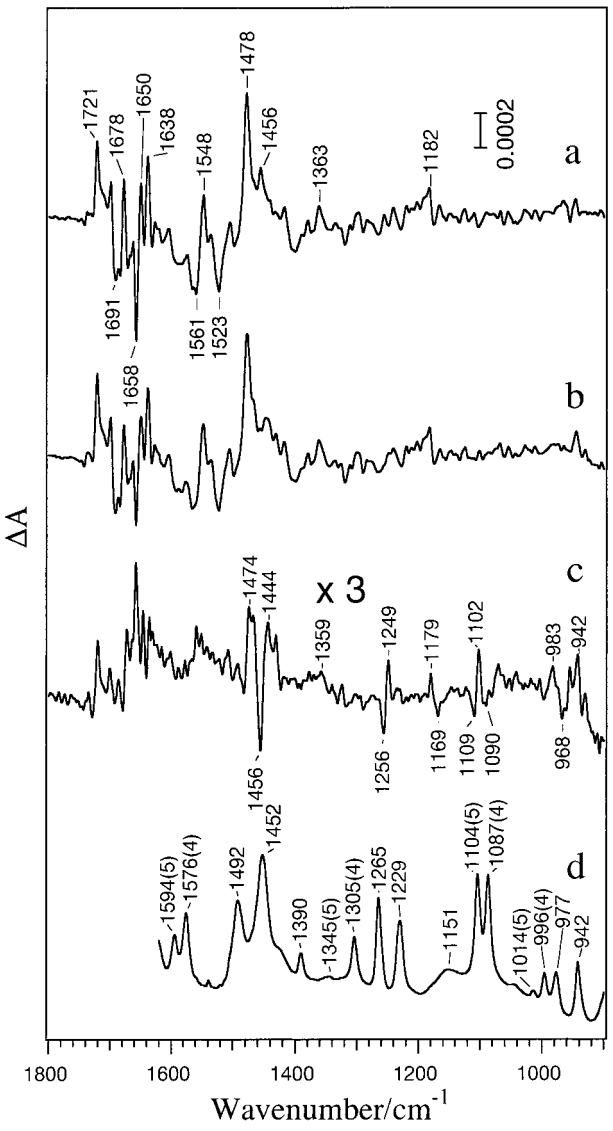

FIGURE 1: Light-induced Q_A^-/Q_A FTIR difference spectra of the Mn-depleted PS II core complexes from unlabeled cells of *Synechocystis* PCC 6803 (a) and from cells in which both of the two imidazole nitrogens of His residues are selectively labeled with ^{15}N (b). The sample contains NH_2OH as an exogenous electron donor and DCMU to block electron flow beyond Q_A. The spectrum was measured at 250 K. (c) Difference between unlabeled and [^{15}N]-His-labeled Q_A^-/Q_A spectra (b − a). The spectral scale is 3 times larger than that of spectra a and b. (d) FTIR spectrum of 4- and 5-methylimidazole dissolved in H_2O. 4- and 5-MeIm are in tautomeric equilibrium in aqueous solution. The spectrum was measured at room temperature. The background due to water absorption was eliminated by subtraction of a spectrum of water. The region above 1620 cm^{-1} is not shown because of the remaining water band, but no bands due to 4- and 5-MeIm are observed. The numbers 4 and 5 in parentheses indicate that the bands have been specifically assigned to 4- and 5-MeIm, respectively (*23*).

coupled to Q_A. To ascertain that the corresponding modes in fact exist in the His vibrations, FTIR spectra of 4- and 5-MeIm, model compounds of the His side chain, were measured in aqueous solution (Figure 1d). 4- and 5-MeIm are in a tautomeric equilibrium in aqueous solution with respect to the protonation site on the two nitrogens (*23*). In the case of a His side chain, N_τ- and N_π-protonated states correspond to 4- and 5-MeIm, respectively. Numerous bands are observed in the 900−1600 cm^{-1} region in Figure 1d; some bands have been assigned specifically to 4- or 5-MeIm (indicated as 4 or 5 in parentheses in Figure 1d, respectively) (*23*, *24*), and others are common for both 4- and 5-MeIm or closely overlap each other. Although the spectrum in the region of > 1600 cm^{-1} is not shown because of the substantial change of the baseline left after subtraction of water absorption, no band of 4- and 5-MeIm was present in this region.

The signal at 1474/1456/1444 cm^{-1} in the double-difference spectrum (Figure 1c) may correspond to the band-(s) at 1452 and/or 1492 cm^{-1} of 4- and 5-MeIm (Figure 1d). The weak feature at 1359 cm^{-1} (Figure 1c) might correspond to the 1345 cm^{-1} band characteristic of 5-MeIm. The clear differential signal at 1256/1249 cm^{-1} (Figure 1c) is a counterpart of the 1265 cm^{-1} band of 4- and 5-MeIm. The signal at 1179/1169 cm^{-1} (Figure 1c) corresponds to the relatively broad band at 1151 cm^{-1} (Figure 1d). This band in 4- and 5-MeIm has been assigned to the mode including the NH bending vibration, and the frequency upshift has been observed upon strong hydrogen bonding (*23*). For instance, in polycrystalline 4-MeIm, the band is found at 1191 cm^{-1} (*23*). The band position at 1179 cm^{-1} in the PS II core proteins (the other peak at 1169 cm^{-1} is from [^{15}N]His), which is 28 cm^{-1} higher than that of 4- and 5-MeIm in aqueous solution, suggests that the His side chain coupled to Q_A is strongly hydrogen bonded. The signal at 1109/1102/1090 cm^{-1} in the double-difference spectrum (Figure 1c) corresponds to the band at 1104 cm^{-1} of 5-MeIm. (The lower-frequency peak at 1090 cm^{-1} arises from [^{15}N]His, and thus, the peaks at 1109/1102 cm^{-1} can be compared to 4- and 5-MeIm.) Together with the weak signal at 1359 cm^{-1} (Figure 1c), the presence of bands characteristic of 5-MeIm suggests that the Q_A-coupled His residue is N_π-protonated. Also, the signals at 983/968 and 942 cm^{-1} may be counterparts of 977 and 942 cm^{-1} bands, respectively, of 4- and 5-MeIm. Some of the bands of 4- and 5-MeIm, e.g., bands at 1594/1576, 1390, 1229, and 1014/996 cm^{-1}, did not show corresponding bands in the double-difference spectrum of Q_A^-/Q_A. This is consistent with the result of normal mode calculation (*23*) that these bands are assigned to the modes in which vibrations of the nitrogen atoms have no or very small contributions.

Figure 2b shows a Q_A^-/Q_A difference spectrum measured using the PS II core complexes from *Synechocystis* cells in which Trp residues are labeled with Trp-d_5. The spectrum was virtually identical to the Q_A^-/Q_A spectrum of the unlabeled PS II core (Figure 2a). This is verified by taking a difference of the two spectra (Figure 2c). No band beyond the noise level was observed. Thus, Trp bands are not detected in the Q_A^-/Q_A spectrum, indicating that structural coupling between Q_A and a Trp side chain, if any, is rather weak.

When an NH group of imidazole compounds is involved in strong hydrogen bonding, a broad NH stretching band appears around 2800 cm^{-1} with a number of sub-bands, while a free NH group shows a narrow band at about 3500 cm^{-1} (*23*, *25*−*28*). These sub-bands have been explained to arise from the Fermi resonance of overtones or combinations of fundamental vibrations with the superimposing NH stretching vibration (*25*−*27*). Figure 3 shows the hydrogen-bonding NH stretching region (2500−3000 cm^{-1}) of Q_A^-/Q_A difference spectra. The spectrum of unlabeled PS II core complexes (Figure 3a) shows several peaks at 2611, 2704, 2758,

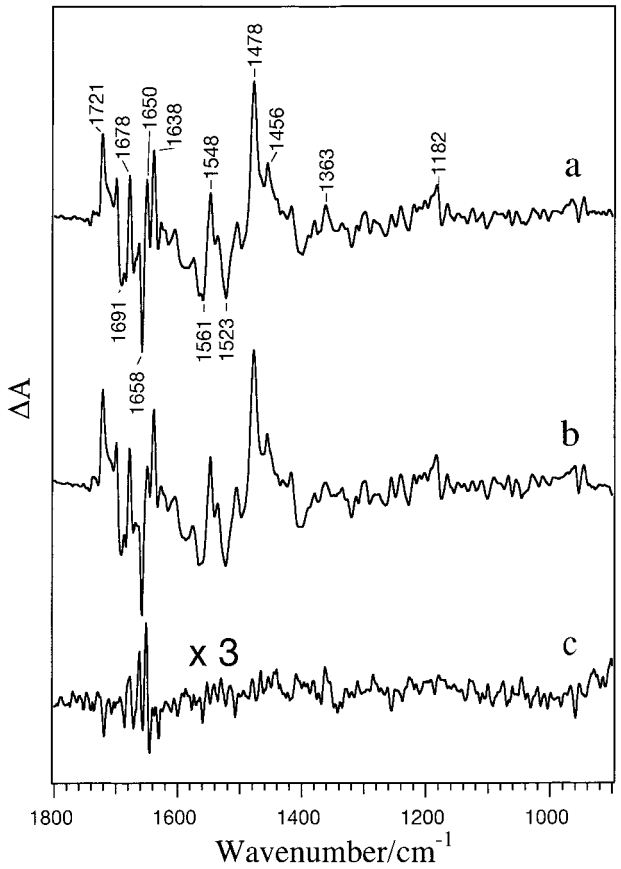

FIGURE 2: Q_A^-/Q_A FTIR difference spectrum of the Mn-depleted PS II core complexes from unlabeled *Synechocystis* cells (a) and from cells in which Trp side chains are selectively replaced with Trp-d_5 (b). The measuring conditions were the same as those described for panels a and b of Figure 1. (c) Difference between unlabeled and Trp-d_5-labeled Q_A^-/Q_A spectra (b − a).

2813, and 2940 cm^{-1}. This feature did not change in the Trp-d_5-labeled PS II core (Figure 3b). Upon [^{15}N]His labeling, however, all the peaks were downshifted by 7−29 cm^{-1}, indicating that these peaks arise from vibrational modes of the His side chain coupled to Q_A. It is considered that these are the sub-bands on the NH stretching vibration that is involved in strong hydrogen bonding. Different extents of downshifts of individual peaks upon [^{15}N]His labeling are reasonably explained by the Fermi resonance of overtones or combinations of various fundamental modes.

DISCUSSION

An FTIR difference spectrum of Q_A upon its photoreduction exhibits not only the bands of Q_A but also the bands of the surrounding protein moiety affected by the Q_A reduction. Analysis of these protein bands provides information about interaction between Q_A and the protein that may play an important role in the reaction mechanism. In this study, several His bands in the Q_A^-/Q_A spectrum were identified by measuring a spectrum using [^{15}N]His-labeled PS II core complexes (Figures 1 and 3), demonstrating the presence of coupling between Q_A and the nearby His residue. Strong hydrogen bonding of the imidazole NH of this His was shown by (i) the presence of several peaks at 2600−3000 cm^{-1} (Figure 3), which arise from the Fermi resonance of harmonics or combinations of imidazole modes with the NH stretching vibration involved in strong hydrogen bonding

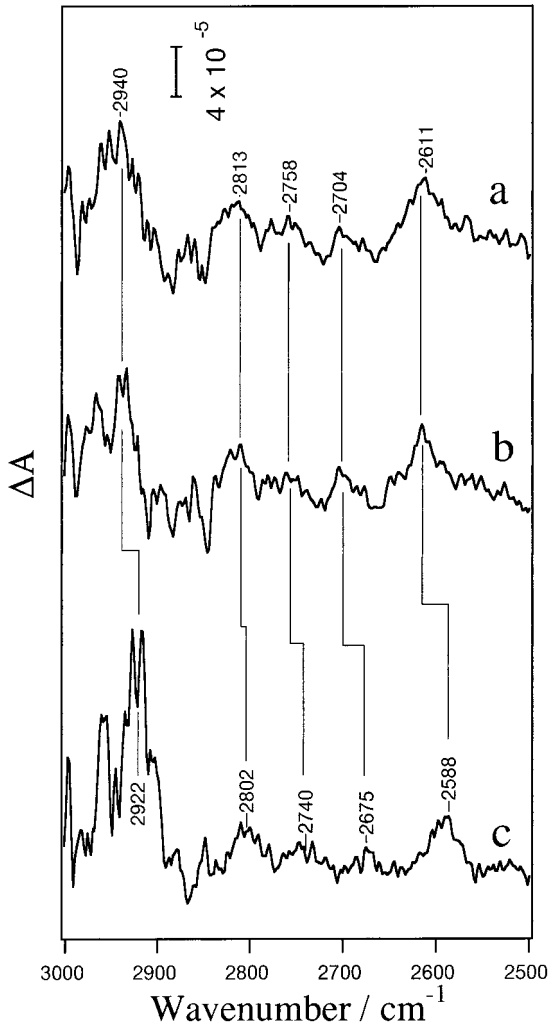

FIGURE 3: Hydrogen-bonding NH stretching region of Q_A^-/Q_A spectra: (a) unlabeled PS II core complex, (b) Trp-d_5-labeled PS II core complex, and (c) [^{15}N]His-labeled PS II core complex.

(*25*−*27*), and (ii) the 1179 cm^{-1} band (Figure 1c), which can be assigned to the mode including NH deformation (*23*), being at a frequency significantly higher than the corresponding 1151 cm^{-1} band of 4- and 5-MeIm in aqueous solution (Figure 1d). Also, the presence of the bands specific to the N_π-protonated state (5-MeIm as a model compound) at 1109/1102/1090 and 1359 cm^{-1} (Figure 1c) suggests that the Q_A-coupled His is protonated at the N_π site. These results are in good agreement with the model of Q_A interaction, which is based on the bacterial structure (*2*, *3*), in which His215 (D2), which coordinates to the non-heme iron at N_τ, is hydrogen bonded to the Q_A carbonyl through the N_π−H bond (*29*). This view is also consistent with our recent FTIR data which show that His modes in the Q_A^-/Q_A spectrum were affected by non-heme iron depletion (*30*); a double-difference spectrum of Q_A^-/Q_A between untreated and non-heme iron-depleted PS II membranes from spinach showed bands at 1367/1336, 1251, 1183, and 1105/1093 cm^{-1} corresponding to the His bands at 1359, 1256/1249, 1179/1169, and 1109/1102/1090 cm^{-1} observed in this study (Figure 1c). Magnetic coupling of Q_A^- with an imidazole nitrogen has been suggested by ESEEM studies using PS II samples treated to decouple the magnetic interaction with high-spin Fe^{2+} (*9*, *11*, *12*, *14*, *15*). However, definitive evidence of specific isotope labeling of His has not been

provided. It is worth noting that the results of this FTIR study were obtained using "intact" PS II core complexes without any special treatment, and definitive identification of the His modes was provided by specific labeling of His side chains.

In contrast to His, no bands of Trp side chains were detected in the Q_A^-/Q_A spectrum by Trp-d_5 labeling (Figure 2). In the bacterial reaction center, a Trp residue (M252 in *Rhodobacter sphaeroides*) is present in van der Waals contact with Q_A (*2*, *3*). In PS II, the corresponding Trp residue, Trp254 (D2), is conserved and thus is supposed to interact with Q_A through $\pi-\pi$ interaction (*4*, *29*). In this FTIR study, however, we could not detect structural coupling between Q_A and a Trp side chain. Probably, the predicted $\pi-\pi$ interaction is not strong enough to influence the vibrations of the indole ring of Trp upon Q_A reduction. Alternatively, Trp254 (D2) is located rather far from Q_A in PS II compared with the bacterial case. This conclusion, however, does not necessarily contradict the importance of Trp254 (D2) in binding of Q_A and its function, which has been demonstrated by site-directed mutagenesis (*31*). FTIR is not quite sensitive to weak electronic interaction that may be important to molecular binding in the protein as well as in an electron transfer reaction.

In conclusion, the FTIR study showed that a His side chain is strongly hydrogen bonded to Q_A through the imidazole NH, demonstrating that the Q_A−His interaction in the bacterial reaction center is conserved in PS II. This hydrogen-bonding structure may be important in controlling the redox potential of Q_A, which is essential to the Q_A function as an electron acceptor from pheophytin and an electron donor to Q_B.

ACKNOWLEDGMENT

We thank Dr. R. D. Britt for providing [^{15}N]histidine.

REFERENCES

1. Diner, B. A., and Babcock, G. T. (1996) in *Oxygenic Photosynthesis: The Light Reactions* (Ort, D. R., and Yocum, C. F., Eds.) pp 213−247, Kluwer, Dordrecht, The Netherlands.
2. Allen, J. P., Feher, G., Yeates, T. O., Komiya, H., and Rees, D. C. (1988) *Proc. Natl. Acad. Sci. U.S.A. 85*, 8487−8491.
3. Emler, U., Fritzsch, G., Buchanan, S. K., and Michel, H. (1994) *Curr. Biol. 2*, 925−936.
4. Michel, H., and Deisenhofer, J. (1988) *Biochemistry 27*, 1−7.
5. Klimov, V. V., Dolan, E., Shaw, E. R., and Ke, B. (1980) *Proc. Natl. Acad. Sci. U.S.A. 77*, 7227−7231.
6. MacMillan, F., Lendzian, F., Renger, G., and Lubitz, W. (1995) *Biochemistry 34*, 8144−8156.
7. Akabori, K., Kuroiwa, S., and Toyoshima, H. (1992) in *Research in Photosynthesis* (Murata, N., Ed.) Vol. II, pp 123−126, Kluwer, Dordrecht, The Netherlands.
8. Sanakis, Y., Petrouleas, V., and Diner, B. A. (1994) *Biochemistry 33*, 9922−9928.
9. Deligiannakis, Y., Jegerschöld, C., and Rutherford, A. W. (1997) *Chem. Phys. Lett. 270*, 564−572.
10. Tang, X.-S., Peloquin, J. M., Lorigan, G. A., Britt, R. D., and Diner, B. A. (1995) in *Photosynthesis: from Light to Biosphere* (Mathis, P., Ed.) Vol. I, pp 775−778, Kluwer, Dordrecht, The Netherlands.
11. MacMillan, F., Kurreck, J., Adir, N., Lendzian, F., Käss, H., Reifarth, F., Renger, G., and Lubitz, W. (1995) in *Photosynthesis: from Light to Biosphere* (Mathis, P., Ed.) Vol. I, pp 659−662, Kluwer, Dordrecht, The Netherlands.
12. Astashkin, A. V., Kawamori, A., Kodera, Y., Kuroiwa, S., and Akabori, K. (1995) *J. Chem. Phys. 102*, 5583−5588.
13. Deligiannakis, Y., Boussac, A., and Rutherford, A. W. (1995) *Biochemistry 34*, 16030−16038.
14. Renger, G., Kurreck, J., Haag, E., Reifarth, F., Bergmann, A., Parak, F., Garbers, A., MacMillan, F., Lendzian, F., and Lubitz, W. (1997) in *Bioinorganic Chemistry* (Trautwein, A., Ed.) pp 260−277, VCH, Tokyo.
15. Astashkin, A. V., Hara, H., Kuroiwa, S., Kawamori, A., and Akabori, K. (1998) *J. Chem. Phys. 108*, 10143−10151.
16. Rigby, S. E. J., Heathcote, P., Evans, M. C. W., and Nugent, J. H. A. (1995) *Biochemistry 34*, 12075−12081.
17. Berthomieu, C., Nabedryk, E., Mäntele, W., and Breton, J. (1990) *FEBS Lett. 269*, 363−367.
18. Noguchi, T., Ono, T., and Inoue, Y. (1992) *Biochemistry 31*, 5953−5956.
19. Hienerwadel, R., Boussac, A., Breton, J., and Berthomieu, C. (1996) *Biochemistry 35*, 15447−15460.
20. Tang, X.-S., Diner, B. A., Larsen, B. S., Gilchrist, M. L., Lorigan, G. A., and Britt, R. D. (1994) *Proc. Natl. Acad. Sci. U.S.A. 91*, 704−708.
21. Barry, B. A., and Babcock, G. T. (1987) *Proc. Natl. Acad. Sci. U.S.A. 84*, 7099−7103.
22. Tang, X.-S., and Diner, B. A. (1994) *Biochemistry 33*, 4595−4603.
23. Majoube, M., Millié, Ph., and Vergoten, G. (1995) *J. Mol. Struct. 344*, 21−36.
24. Ashikawa, I., and Itoh, K. (1979) *Biopolymers 18*, 1859−1876.
25. Wolff, H., and Wolff, E. (1971) *Spectrochim. Acta 27A*, 2109−2118.
26. Perchard, C., and Novak, A. (1968) *J. Chem. Phys. 48*, 3079−3084.
27. Bellocq, A. M., Perchard, C., Novak, A., and Josien, M. L. (1965) *J. Chim. Phys. 62*, 1334−1343.
28. Zimmermann, H. (1961) *Z. Elektrochem. 65*, 821−840.
29. Diner, B. A., Petrouleas, V., and Wendoloski, J. J. (1991) *Physiol. Plant. 81*, 423−436.
30. Noguchi, T., Kurreck, J., Inoue, Y., and Renger, G. (1999) *Biochemistry* (submitted for publication).
31. Vermaas, W., Charité, J., and Shen, G. (1990) *Z. Naturforsch. 45c*, 359−365.

BI982294V